Light Metals 2012 *Edited by: Carlos E. Suarez*
TMS (The Minerals, Metals & Materials Society), 2012

Study of Ni-Impurity Removal from Al Melt

M.A. Rhamdhani[1], M.A. Dewan[2], J. Mitchell[3], C.J. Davidson[3], G.A. Brooks[1], M. Easton[4], J.F. Grandfield[5]
CAST Cooperative Research Centre (CAST CRC), Australia
[1]Swinburne University of Technology, Melbourne, VIC 3122, Australia
[2]CSIRO Materials Science and Engineering, Australia
[3]CSIRO Process Science and Engineering, Australia
[4]Monash University, Clayton, VIC 3800, Australia
[5]Grandfield Technology Pty Ltd, Brunswick West, VIC 3055, Australia

Keywords: Al impurities, nickel removal, iron removal, Al refining

Abstract

Impurity control in the production of Al alloys is very important for achieving desired alloy properties. There has been an increasing impurity concentration (particularly nickel and vanadium) in the coke used in the primary Al production which ends up in the Al alloys. V can be removed in the casthouse through boron treatment. Ni, however, is a non-reactive element and difficult to be remove. There is currently no technique available in the casthouse to remove Ni. The current paper describes an exploratory study of Ni removal from Al melt. A literature review on the available techniques for the removal of Ni impurity from Al melt was carried out; followed by a systematic thermodynamic analysis of various Al-Ni-X systems for possible formation of Ni-containing phases in Al melt. Laboratory experiments were carried out to test the possible systems identified from the thermodynamic analysis.

Introduction

The control and removal of impurities from Al melt has become an important topic in a greater range of alloys as impurity levels are rising both in the primary production process and through increased recycling. The impurities of Al from the primary production process are limited by the impurities in raw materials used and to some extent from the construction materials and operation of the smelting unit. It has been reported that there is an increase in Ni and V concentrations in the smelter grade Al that mostly come from the petroleum coke in the carbon anodes used in the preceding Hall-Heroult process [1]. As sweet crude becomes scarcer and more sour crude is used in petroleum coke production, levels of Ni and V in coke have steadily risen in the last decade (~10-20 ppm per annum [2-4]). Green cokes of 600 ppm V are routinely being blended into the calcined coke supply and levels may go as high as 1000-2000 ppm at some stage in the future.

Grandfield *et al.* [5] pointed out that interventions can be made at each stage of the value chain for better control of impurities. In the case of Ni and V, this includes development of methods for removing these impurities in the casthouse. V can be removed in the casthouse using boron/boride treatment. Currently, there is no technique in the casthouse for removing Ni. The current paper focuses on the exploratory study of Ni removal from Al melt. The approach taken includes: literature study on various methods for removing impurities; systematic thermodynamic analysis of various Al-Ni-X systems for possible formation of Ni-containing phases in Al melt; followed by laboratory tests of the system identified in the thermodynamic study.

Available Ni Removal Techniques

The literature review carried out in this study indicates that there is no currently available technique for removing Ni from Al melts in the casthouse. There are, however, techniques for producing ultrapure Al, i.e. purity of greater than 99.99%, as summarized by Dewan *et al.* [6]. These processes are not widely used in the Al industry. Nevertheless, they may provide some guideline for conventional impurity removal techniques and development of new techniques particularly for non-reactive metals such as Ni and Fe. Each process is explained in more details in the following subsections:

Three-Layers Electrolytic Method

This process consists of an electrolytic cell having three liquid layers – two molten Al layers separated by a salt or electrolyte layer. The bottom layer in the cell is the impure Al alloy layer (e.g. Al-Cu alloy) that forms the anode and is purified by electrolytically transferring Al through the intermediate salt layer to the top layer of high purity molten Al (the cathode) [7-8]. Al produced by three-layer electrolysis has significantly reduced impurity concentrations. This Al product has a very low content of non-reactive impurities, i.e. less than 10 ppm. The three-layer cell is effective in reducing Mn, Cr, Ti, V, Zr, and Ga contents. Such a cell can also lower the concentration of Si, Fe, Ni and Cu [7-8]. There are three patented processes that based on this method, namely Hoopes process (USA) [9-11], Gadeau process (France) [12], and S.A.I.A (Societe Anonyme pour l'Industrie de l'Aluminium) process (Swiss) [13]. These three processes are the same in principle, with main differences on the type of electrolyte used, the composition of the anode used, and the temperature of operation.

Zone Refining Method

High purity Al can also be obtained by the zone refining process [14-16]. This process was developed by Pfann [17-18], and its potential for ultrapurification was first recognised when it was applied to germanium [19]. The process involves applying heat to a section of solid alloy ingot/bar. Only a small portion of the bar is melted and this molten zone is moved slowly from one end to the other. Movement is always in the same direction along its length. The interface between the liquid and solid is maintained to be planar by solidifying at a slow growth rate with a steep temperature gradient [20]. As impurities are usually more soluble in the liquid they are carried forward with the molten zone so that the re-solidified material is purified [21-22]. Zone refining is very effective in reducing the amount of strongly partitioning eutectic elements such as Cu, Fe, Si, and Mg in Al. The effectiveness is much lower for Na and Ca and, as with Cr and Mn, the contents of these impurities in Al seem to be the same after twenty zone

passes as before zone refining [15]. Kino *et al.* [16] studied the purification of Al by zone refining and concluded that the purification saturated at a particular level and further zone passing contaminated the sample. The optimum conditions found in their study for purification were: zone speed of 24~55 mm/hr, zone length less than 30 mm and about 10 passes. Hashimoto *et al.* [23] produced ultra pure Al, 99.99999% repeated zone-passing and cropping 30 to 60 times.

Fractional Solidification Method

Another method used for the purification of Al is referred to as fractional crystallization [24-25]. Refining fractional crystallization is based on the fact that when a melt containing one or more solutes is cooled, crystals that solidify have different impurity content than the liquid. The fractional crystallization technique was commercially practiced at Alcoa to produce extremely pure Al (99.99+ %) [9, 26]. Purification is accomplished by allowing crystallization to initiate at the top surface of molten metal bath and settle to the bottom of the melt bath. This is carried out by controlling the removal of heat at the surface of the molten liquid. The solid crystals (having higher purity) are packed into the bottom of the apparatus and less pure molten Al is withdrawn through an upper exit port to inhibit contamination of the solid, pure Al adjacent to the bottom of the apparatus. Through this process the purity can be upgraded to 99.993% from a starting purity of 99.91% and the eutectic impurities in the final fraction are lowered from 0.083 wt% to 0.006 wt%. However, this process does not remove Ti, Zr, V, Mn, and Cr [7].

Thermodynamics Analysis

In this study, the thermodynamic data of a wide variety of Al-Ni systems (borides, nitrides, sulphides, phosphides, chlorides) were examined to identify a possible Ni compound (simple phases of solid, gas, liquid or complex intermetallics) that might be formed in the melt and removed in subsequent processes (floatation, settling, evaporation, etc). These are presented through the following general reactions;

$$\underline{Ni} + \underline{X} = NiX \text{ (solid, liquid, or gas)} \quad (1)$$

$$\underline{Ni} + MX = \underline{M} + NiX \text{ (solid, liquid, or gas)} \quad (2)$$

where M is desirable alloying elements (e.g. Mg, Si, Zn, Cu). For this study, two packages were used, FactSage 6.2 and HSC Chemistry 7.1, and the work involved:

- Evaluation of the Gibbs energy formation of Ni compounds
- Equilibrium calculations of Ni-Al-X, Ni-Mg-Al, Ni-Mg-Zr-Al, and Ni-V-Al-X (where X = C, F, N, B, P, S and Cl)

Evaluation of the Gibbs Free Energy of Formation

The relative stability of Ni compounds compared to Al compounds can be evaluated by comparing their Gibbs free energy of formation. Table 1 shows the summary of the comparison between ΔG of various Ni-compounds and their associated Al-compounds. It is apparent from Table 1 that only a few compounds of Ni have more negative Gibbs free energy formation compared to their associated Al-compounds. Nickel boride, nickel carbonate ($NiCO_3$) and nickel phosphide (NiP) exhibit a lower Gibbs free energy formation compared to the corresponding Al compounds. Figures 1(a) and 1(b) show the detailed comparison between the Gibbs free energy of formation of Ni-borides and Ni-phosphides to their corresponding Al compounds. It should be noted, however, that the ΔG of these compounds was calculated by assuming pure compounds and without considering the solution behavior of the impurities in Al melt. Therefore these results are indicative. Although the examination of the free energies indicates removal of Ni by boride treatment is a possibility, it does not seem to have been reported in the literature.

Table 1 - Summary of the comparison between ΔG of Ni-compounds with their associated Al-compounds

Type of Compounds	Ni-	Details
Chloride	×	
Chlorate	×	
Fluoride	×	
Carbide	×	
Carbonate	✓	ΔG $NiCO_3$ < ΔG $Al_2(CO_3)_3$ (below 600°C)
Nitride	×	
Nitrate	×	
Sulphide	×	
Sulphate	×	
Hydride	×	
Iodide	×	
Iodate	×	
Boride	✓	ΔG Ni_3B < ΔG AlB_2 < ΔG AlB_{12}
Phosphide	✓	ΔG Ni_3P < ΔG AlP
Phosphate	×	

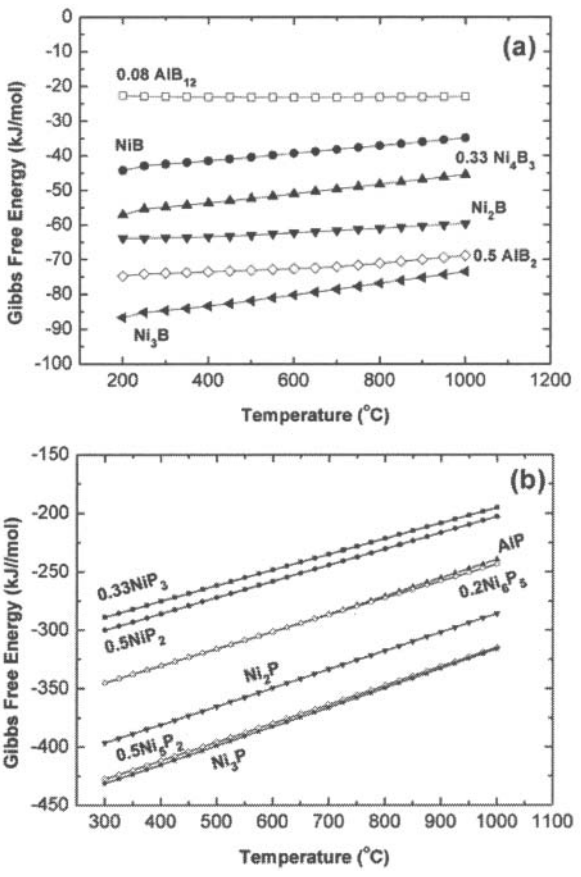

Figure 1. Gibbs free energy formation comparison between: (a) Ni-borides and Al-borides; and (b) Ni-phosphides and Al-phosphide

Equilibrium Calculations of Ni-Al Systems Reacted with Various Potential Additives

Equilibrium calculations (taking into account the solution behavior of the impurities) were carried out to investigate the effect of the potential additives on the Ni in the Al melt. The equilibrium calculations were carried out using FactSage 6.2 for the Ni-Al system at temperatures of 650°C to 950°C, with various potential additives such as C, F, N, B, P, S and Cl (100 to 300 ppm). The Ni concentration of 80 ppm was used for the calculations as this was the typical Ni concentration of commercial Al melt.

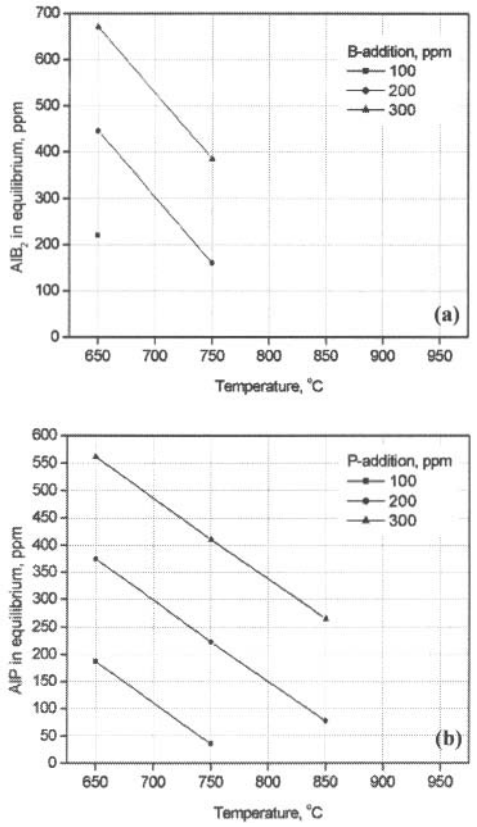

Figure 2. Predicted equilibrium concentration of solid phases formed after (a) boron and (b) phosphorus addition (100-300 ppm) into Al-Ni (80 ppm) melt. Only AlB_2 and AlP phases predicted to form.

Figures 2(a) and 2(b) show the predicted solid phases formed when B and P were added (100 to 300 ppm) into the Al melt containing 80 ppm Ni at 650°C to 950°C. In both cases no Ni solid phases were predicted to form at the temperatures studied. Rather, the phosphorus and boron react with Al to form AlP and AlB_2. The concentrations of solid AlP and AlB_2 increased with increasing amount of P and B additions, respectively. The stability of AlP and AlB_2 depends on the temperature. As the temperature increases, both AlP and AlB_2 dissociate and dissolve into the Al melt. No solid phases were observed above 850°C (for Al-Ni melt) and 950°C (for Al-V melt), i.e. all elements are in solution with liquid Al. In the temperature and composition range studied, the equilibrium calculations predicted that no Ni-containing solid phases are formed when B, P, C, F, N, S and Cl are added to the Al-Ni melt.

Further equilibrium calculations were carried out at higher concentrations of Ni to investigate the possible formation of Ni-containing phases. These include calculations on the following systems: Al-Ni-V-S; Al-Ni-V-P; Al-Ni-V-N; Al-Ni-V-Cl; Al-Ni-V-C; Al-Ni-V-B; Al-Ni-V-$Na_2B_4O_7$; at temperatures 700 to 900°C. In all cases, no solid/gas/liquid phases of Ni were predicted to form at equilibriums for the conditions studied. Ni was predicted to form as solute within the Al melts. The additives were predicted to react with Al forming Al-compounds, e.g. AlS, AlP, $NaAlO_2$, AlN, Al_4C_3, AlB_2, $Na_2Al_{12}O_{19}$.

In summary, the Gibbs free energy evaluation suggests two potential additives that may be used for removing Ni from the Al melt, i.e. B, and P for the formation of Ni-borides and Ni-phosphides. However, the equilibrium calculations predicted that no Ni-containing phases are formed when B and P are added. This may be due to the dilute concentrations of Ni in the Al melt. To confirm the findings from the thermodynamic study, experimental work using the Al-Ni-P and Al-Ni-B systems were carried out. In addition two systems, Al-Ni-Zr and Al-Ni-Mg-Zr, were also investigated. These systems were chosen to test the finding of Foerster [27] who reported the removal of Ni from Mg melt by addition of Zr and Al at 760°C through the formation of complex Al-Zr-Ni intermetallic. It has also been pointed out that problems associated with Ni in Al seem to be strongly related to Ni in Mg [28]. The details of the experimental work are discussed in the following sections.

Experimental Methodology

An experimental study to explore the possibility of the formation of Ni-containing phases was carried out. The typical Ni concentration in the Al smelter grade is 0.001wt%. However, for the purpose of the current experimental study a greater concentration was used (up to 100 times greater ~ 0.1wt%). This concentration was chosen to increase the likelihood of detection of particles formed. The following alloys and compounds were used to produce the master alloys for the experiments: Al, Al-3 at% Ni, Al-15 at% Zr, Al-4 at% B, Al-10 at% B, and $AlCu_8P_{1.4}$. Table 2 shows the experiments carried out in the present study.

Table 2. Summary of experimental work carried out in the present study; all experiments were carried out at T = 750°C.

Alloy	System	Conc. (wt%)	Other Information
11	Al-Ni-P	0.11 Ni 0.06 P	Target phase Ni_3P
12	Al-Ni-P	0.11 Ni 0.12 P	Target phase: Ni_3P
12X	Al-Ni-P	0.11 Ni 0.06 P	Repeat (increased standing time and slow cooling); Target phase Ni_3P
12XX	Al-Ni-P	0.11 Ni 0.06 P	Repeat (covered by salt flux) Target phase Ni_3P
21	Al-Ni-Zr	0.11 Ni 0.17 Zr	Target phase: Al-Ni-Zr intermetallic
22	Al-Ni-Zr	0.11 Ni 0.34 Zr	Target phase: Al-Ni-Zr intermetallic
41	Al-Ni-Mg-Zr	0.16 Mg 0.008 Ni 0.16 Zr	Target phase: Mg-Ni-Zr intermetallic
31	Al-Ni-B	0.109 Ni 0.17 B	Target phase: Ni_3B
32	Al-Ni-B	0.109 Ni 0.34 B	Target phase: Ni_3B

The experiments were carried out at 750°C. For each experiment, 1kg of metal was melted in an induction furnace and from each melt the following samples were taken:

- 1 quenched sample (designated as "Q"); a small sample was scooped from the melt in a ladle and quenched into water.
- 1 "slow-cooled" sample (designated as "S"), in a graphite mould with an insulating lid (cooling rate approximately 1°C /s) – filled via ladle from the melt.
- 1 wedge sample ~700g (designated as "W"), cooled in a copper mould with a wedge-shaped cavity and with insulated ends. This allows a wide range of liquid cooling rates, from approximately 1°C/s at the top ("WT") to about 100°C/s at the base ("WB").
- A "remelt" sample (designated as "R"), where a section of the wedge casting (~ 150g), was remelted and increased slowly to 750°C, held for 1 hour, and then allowed to cool in the furnace. Solidification occurred at approximately 2°C /min.

All combinations of alloy and solidification conditions were prepared and examined by optical metallography. Selected samples were then examined by scanning electron microscopy, energy dispersive X-ray analysis (EDS) and optical emission spectroscopy (OES). The EDS system that was used provides a standardless quantitative mode. The reproducibility was good, and small relative differences can be identified, but the absolute accuracy was less well characterised. Additionally, minor phases were often of the order of 1μm in size, creating further inaccuracies in quantitative analysis. All phase compositions should be interpreted in the light of these limitations and any phase identification in this study was also based on the nearest likely known intermetallic phase from the phase diagrams and thermodynamic databases.

Results and Discussions

Al-Ni-P (Alloys 11 and 12)

The microstructures of Alloys 11 and 12 (had a nominal 0.06 and 0.12 wt% P, respectively) were similar, except for minor phase fractions. The minor phases were very fine and mainly intergranular, although there were also some tiny globules in the interdendritic regions. The Ni-rich phase was almost continuous along grain boundaries and some grains had tiny interdendritic globules, while other grains appeared devoid of these. This variability might have been due to variations in dendrite morphology within grains, or simply related to random planes of section not intersecting any globules. The globules were mainly Al, but also had significant Ni, with varying smaller amounts of Fe and Cu.

The microstructures of slow-cooled (S), wedge-top (WT) and wedge-base (WB) samples were very similar, and in both samples the phases were consistent with analyses from the quenched (Q) sample. Slow cooling of the remelt sample (R) allowed coarser microstructures to evolve and permitted resolution of the minor components as different phases. The most common two minor phases that were identified were $Al_2(Cu,Ni)$ and $Al_n(Ni,Fe)$. A small amount of Al_3Ni was also noted. Evaluation of the thermodynamic database revealed the closest intermetallics would have been $Al_9(Fe,Ni)_2$ and $Al_3(Ni,Cu)_2$. Figure 3(a) shows the backscattered secondary electron images of minor phases at the grain boundary. These Ni containing phases do not appear to form prior to solidification.

In order to try to identify the phase to which the P reports, two slices were taken from a wedge casting of Alloy 11. One was surveyed with repeated spark analyses, while the other was polished for microscope examination, both optical and SEM. The OES spark analyses showed a relatively uniform distribution of P, Cu and Ni. Some regions with some undissolved Cu_3P (source of P added to the melt) are observed. Isolated Cu_3P particles were identified by optical and scanning electron microscopy. A few Ni-containing particles (Ni_xP) were observed. An example of the largest of Ni_xP particle observed is shown in Figure 3(b).

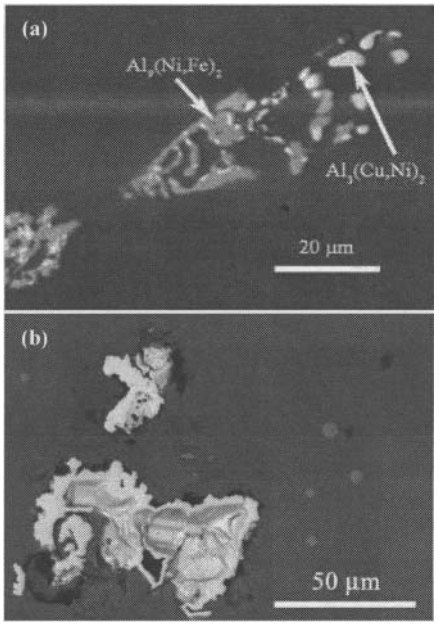

Figure 3. Backscattered electron images of Al-Ni-P samples showing: (a) Grain boundary eutectic and other minor phase clustering; (b) the largest particles of Ni_xP observed

A repeat experiment with increased standing time and slow cooling (Alloy 12X) was carried out to determine if more time was required for equilibrium dissolution and subsequent resulting reactions in the melt to form the target phases. The OES results indicated that P was somewhat under specification at first but rising with the Cu as the Al-Cu-P master alloy becomes fully dissolved after 15 minutes. This indicates that the large particles of Cu_3P observed in the previous experimental study take time to dissolve before liberating P to the melt. The sparks also suggest a slight trend in the P, where larger quantities were obtained at the top of the samples, perhaps pointing towards a migration upwards due to favourable vaporisation or oxidation.

Figures 4(a) and 4(b) show the backscattered electron micrographs from the samples of repeat experiments. Similar structures to that in the previous round of testing were observed. The Al matrix is partitioned at the grain boundaries by $Al_x(Ni, Fe)$ and $Al_x(Cu,Ni)$ phases consisting of varying amounts of Ni, Fe and Cu. A few other eutectic structures exist away from the grain boundaries, also of the same compositions. No isolated Cu_3P nor Ni_xP particles were found as before, suggesting that these particles had re-dissolved due to the longer dissolution time available.

Further experiments were carried out to determine if there is loss of P due to vaporization or sublimation during preparation of the melt in the induction furnace. Two Al-Ni-P alloys (Alloy 12XX) were prepared under a eutectic flux mixture of 44% NaCl and 56% KCl. After the tests the composition of the flux was analysed using ICP to determine P pick up. In addition to the use of flux, the alloys was prepared in a top opening box furnace in order to eliminate the possibility of transport of P to the surface of the melt by the stirring action of the induction furnace. The alloys were prepared by melting Al and then alloying with Al-5%Ni and Al-Cu-P additions wrapped in Al foil to minimize any loss of P. In this experiment the target phase is Ni_3P. The result of the chemical analysis of the NaCl-KCl salt showed a P level of 0.011wt%. This, coupled with a poor recovery of P in the casting suggests a short residence time of P in the melt insufficient to allow reaction with Ni.

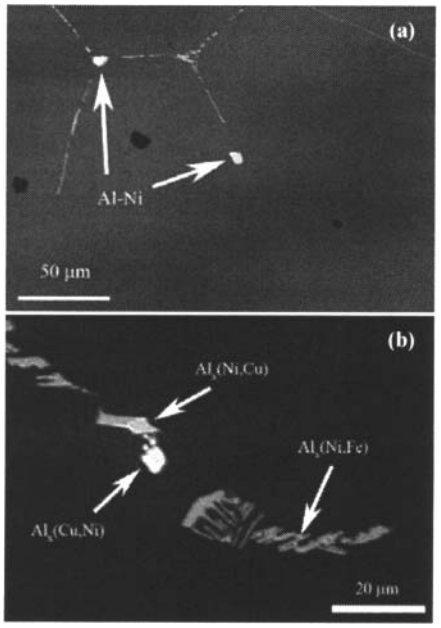

Figure 4. Backscattered electron images of Al-Ni-P samples showing: (a) Typical structure showing Al matrix and Al_x(Ni,Fe) intergranular phase, just after alloying (0 min); (b) typical phases present after 60 mins.

In summary, Ni in the microstructure was found mainly in $Al_9(Fe, Ni)_2$ and $Al_3(Ni, Cu)_2$, both of which precipitate only at the end of solidification. Particles containing only Ni and P (presumably Ni_3P) were observed in the wedge section in the initial experiments. These were large particles, unevenly distributed in the matrix, which gives the impression of a phase that formed in the melt, before primary Al solidification. These were not observed in the repeat experiments with increased standing time and with salt flux covers indicating that the Ni_xP particles formed were a metastable phase or re-dissolved into the Al melt in an extended period of heating time. The short residence time of P in the Al melt maybe insufficient to allow reaction with Ni.

Al-Ni-Zr (Alloys 21 and 22) and Al-Ni-Mg-Zr (alloy 41)

The microstructures observed in the Alloys 21 and 22 were similar, except that the richer alloy had a larger fraction of minor phases. Almost all second phase appears as regular or divorced eutectic in the intergranular regions. Some globular phases were also observed within the grains. The wedge base sample seems to have a greater fraction of Ni-bearing phases present as globules within each grain.

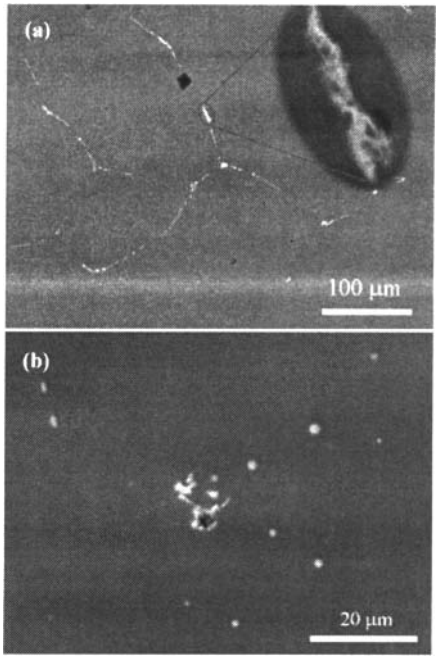

Figure 5. Backscattered electron images of Al-Ni-Zr alloy: (a) Sample 21S showing typical Al-Ni,Fe intermetallics with enlarged inset showing Zr-bearing phase; (b) Sample 22WB showing two distinct eutectic morphologies: small globular phases and grain boundary forms.

SEM and EDS analyses showed that most intermetallics were $Al_9(Fe, Ni)_2$, although a small proportion of Al_3Ni was observed. Zr-bearing phases were difficult to distinguish (in the images and in the SEM) from the far more common Al-Ni,Fe intermetallic phase(s). Figure 5(a) shows a BSE image of a minor phase at the grain boundary. Higher magnification images revealed more complex structures. The EDS spectra showed some degree of association between Zr and Ni, although the instance where Zr concentration was highest had no detectable Ni. Figure 5(b) shows the two distinct eutectic morphologies, i.e. the small globular and intergranular phases. The globular particles were analysed and all contained similar amounts of Ni and Fe, as did the intergranular particles. These were probably very fine eutectic, although many cases were difficult to resolve. Very few Zr-bearing particles were detected. The particle shown in Figure 5(b) was analysed in several places and the Zr content seemed quite consistent. On the other hand, the Ni levels detected in the same spectra varied widely. It cannot be determined whether the analyses with higher Ni levels were due to Ni in the same phase as the Zr, or in adjoining phases at or below the sample surface.

Foerster [27] removed Ni in Mg melt by adding Zr (up to 30 times the amount of Ni) and aluminium (up to 20 times the amount of Ni) to the melt at 760°C. An insoluble Zr-Al-Ni ternary phase in the molten magnesium was formed and further removed by settling. In the current study, both Mg and Zr were added to the previously prepared Al-Ni master alloy in an effort to determine the possibility of forming a ternary Zr-Al-Ni phase in the presence of Mg.

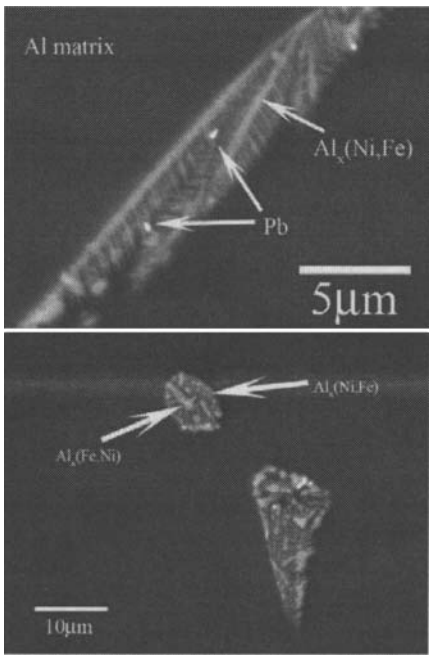

Figure 6. Backscattered electron micrograph of various $Al_x(Ni,Fe)$ particles found in the Al-Ni-Mg-Zr alloy.

Similar microstructures to the Al-Ni-Zr alloys were obtained. Secondary phases containing Zr were difficult to distinguish. Globular eutectic particles of size 3 to 5μm, presumably mostly $Al_9(Fe,Ni)_2$ were observed throughout the sample, many of which form regular linear patterns with one another within the alloy. This may suggest they have formed between dendrite arms. Various interesting morphologies of the $Al_x(Ni,Fe)$ phases are shown in Figure 6. The only other readily detectable element present was Pb (minor contaminant of master alloy). The thermodynamic package predicted that Al_3Zr should start to precipitate out on cooling from 700°C however this phase was not found in the SEM studies. This phase may have redissolved in the Al solid. The model did not predict the presence of $Al_9(Ni,Fe)_2$ at this composition of Ni, however it is certainly present under EDS examination. However increasing the amount of Ni slightly to 0.0175wt% indicated that it may precipitate at the very end of solidification, which is consistent with the microstructures seen above. Additionally, the thermodynamic prediction suggested that the addition of Mg drops the liquidus temperature from approximately 650 °C to 639 °C.

In summary, there is a small degree of association between Zr and Ni in both Al-Ni-Zr and Al-Ni-Mg-Zr alloys, but this seems to be in phases that form late in the solidification process, with little scope for settling. The Ni is mainly associated with Fe in late-forming phases presumed to be $Al_9(Ni,Fe)_2$ and Al_3Ni. Therefore little if any Ni has been removed at higher temperatures. The Al-Zr binary system forms a peritectic reaction at the Al-rich end, just above the pure Al melting point. The liquid composition of this reaction is 0.10 wt%, while the Al(Zr) solid solution limit is 0.27wt%. This would suggest that some Al_3Zr should precipitate from the liquid below 700°C, while the remainder will go into solid solution. Some of the precipitated Al_3Zr might also redissolve in the Al solid. This would be particularly likely in the remelted material, which spent a prolonged time at high temperatures after solidification. A Scheil simulation of Al-0.1Ni-0.05Fe-0.17Zr predicted a solidification sequence that matches the observations, although the Scheil assumptions do not permit any solid state reactions. The thermodynamic package predicts that all Al_3Zr formation has completed before any Ni-bearing phases precipitate, so there is no ternary reaction that could account for the minor amounts of Ni associated with the Zr phase. Early precipitation of Al_3Zr is also difficult to reconcile with its presence in the grain boundaries.

Al-Ni-B (Alloys 31 and 32)

The typical microstructures observed in this allow were similar to Al-Ni-Zr alloys, i.e. the second phases were observed as very fine eutectic pockets and as intergranular phases. Figure 7(a) shows the backscattered electron image of Sample 31WB showing the fine eutectic pockets. A small amount of undissolved AlB_{12}, as well as re-precipitated AlB_2 was observed. A cross-section of each wedge sample was analyzed by optical emission spectrometry for concentration profiles. A very strong concentration gradient from bottom to top of the wedge, suggesting that the borides had segregated to the bottom of the wedge.

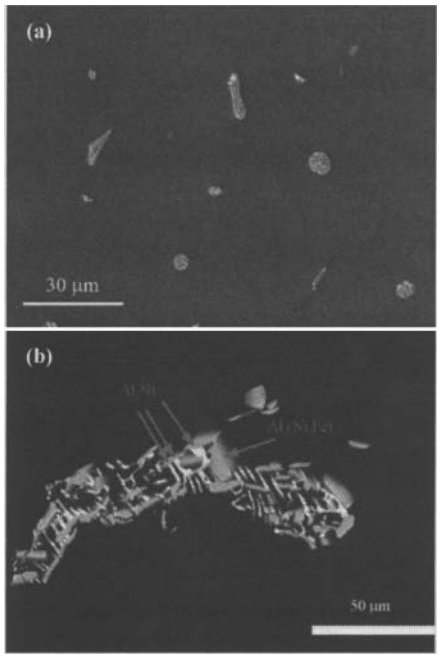

Figure 7. Backscattered electron images of Al-Ni-B alloy: (a) Sample 31WB; showing very fine eutectic pockets; (b) Sample 31R (remelted) showing a complex eutectic region.

All eutectic regions that were examined showed intermetallics of the possible type $Al_n(Fe,Ni)$. The fineness of the phases made accurate measurement impossible, but the Fe:Ni ratio was quite consistent, leading to the interpretation that it was more likely to be a binary eutectic, where Ni and Fe substituted for each other in the intermetallic.

EDS analysis of eutectic/intermetallic particles in Alloy 32 in the samples cast immediately after alloying showed that all were $Al_9(Fe,Ni)_2$ intermetallics, with a slightly variable ratio of Ni:Fe, with Ni always dominant. The coarser phases formed during slower cooling after the remelt experiment allowed individual

particles to be imaged and analysed by EDS. The backscattered-electron image in Figure 7(b) shows clearly that the eutectic is at least a ternary microstructure. The two different intermetallics are clearly distinguishable in this high-contrast image from a very slowly cooled sample.

In summary, the alloys showed some undissolved boride from the master alloy, with Alloy 32 having more in that form than did Alloy 31. B was detected as phases AlB_{12} (remaining from the master alloy) or as AlB_2, in lath or hexagonal form. The AlB_2 gives the appearance of having formed from the liquid, and generally appears within the Al dendrites, rather than as part of the final liquid to solidify. This fits with it being the first solid phase to form Al dendrites then nucleate independently, and randomly capture the AlB_2 as they grow. No Ni was detected in the AlB_2 particles. Ni was always observed in what was presumed to be an $Al_n(Fe,Ni)$ intermetallic, but the coarsest microstructure revealed that there were in fact two intermetallic phases, one almost purely Al-Ni (assumed to be Al_3Ni), and the other with a mix of Fe and Ni, that is probably $Al_9(Fe,Ni)_2$.

Concluding Remarks

In the present work, literature, thermodynamic and experimental studies on Ni removal from Al melt have been carried out and presented. A literature study indicated that there are no techniques available in the casthouse for removing Ni from Al melt. The Gibbs free energy evaluation suggests two potential additives that may be used for removing Ni from the Al melt, i.e. B, and P for the formation of Ni-borides and Ni-phosphides. However, further equilibrium calculations (taking into account the solution behavior) predicted that no Ni-containing phases are formed when B and P are added; rather AlP and AlB_2 are predicted to form. This may be due to the dilute concentrations of Ni in the Al melt. The literature review also revealed the lack of thermodynamic data for dilute solutions in Al melt (particularly that relates to Ni). Further experimental studies of dilute Ni behavior in Al melt are required.

Experimental trials on Al-Ni-P, Al-Ni-B, Al-Ni-Zr, and Al-Ni-Mg-Zr were carried to test the thermodynamic analysis results. In all the trials carried out so far, Ni appeared to remain in the liquid until the later stages of solidification. Upon cooling Ni has invariably precipitated as an Al-Ni intermetallic eutectic phase (divorced or coupled) combined with any available Fe. There are two probable phases, Al_3Ni and $Al_9(Fe,Ni)_2$. In the presence of B, the favoured phase is AlB_2. In the presence of Zr, upon cooling, the elements appear to form separate Al-Zr and Al-Ni intermetallics. In the presence of P, the results may suggest the formation of metastable Ni_xP particles which re-dissolved in Al melt in an extended period of heating time.

The exisiting non-commercialised processes for production of ultra purity Al (such as three-layer electrolysis, zone refining, fractional crystalisation and their combinations) – which have been shown to successfully reduce Ni (and other non-reactive elements such as Fe) in the melt to a very low concentration – may provide some ideas for the development of new techniques in casthouse. It may be possible to integrate an additional process step to the current practices in casthouse that resembles the above techniques for controlling Ni and Fe levels. The presence of Fe in the Al melt also has a role in the precipitation of Ni (formation of Al-Fe-Ni intermetallics). Thus, a removal method that is applicable to Ni will also be applicable for Fe (such as fractional crystallization). It is hoped that the current study provide the basis for further development in this area.

References

1. J.F. Grandfield and J.A. Taylor, "The Impact of Rising Ni and V Impurity Levels in Smelter Grade Al and Potential Control Strategies", *Materials Science Forum*, 630, 2009, pp.129-36.
2. F. Vogt, et al., "A preview of anode coke quality in 2007", *TMS Light Metals*, 2004, pp.489-93.
3. L. Edwards, "Responding to changes in coke quality", *Australian Smelting Conference*, Terrigal, NSW, 2007.
4. V. Danek, et al., "Material balance of vanadium in aluminium reduction cells", *Industrial and Engineering Chemistry Research*, 43 (26), 2004, pp.8239-43.
5. J. Grandfield, et al., "Melt Quality and Management of Raw Material Impurities in Cast House", *10th Australian Aluminium Smelting Technology Conference*, Launceston, Australia, 2011, p.23.
6. M.A. Dewan, et al., "Control and Removal of Impurities from Al Melts: A Review", *Materials Science Forum*, 693, 2011, pp.149-60.
7. R.K. Dawless, and S.C. Jacobs, *Production of Extreme Purity Aluminum*, in *U. S. Patent: 4,222,830*, 1980.
8. R.K. Dawless, and S.C. Jacobs, *Production of Extreme Purity Aluminum*, in *U. S. Patent: 4,239,606*, 1980.
9. R.K. Dawless, et al., "Production of Extreme-Purity Al and Si by Fractional Crystallization Processing", *Journal of Crystal Growth*, 89 (1), 1988, pp.68-74.
10. J.D. Edwards, F.C. Frary, and Z. Jeffries, *The Aluminum Industry, Vol. I. Aluminum and Its Production*, 1930, New York, McGraw-Hill.
11. W. Hoopes, F.C. Frary, and J.D. Edwards, *Electrolytic Production of Aluminum*, in *U. S. Patent: 1,534, 317*, 1922.
12. Cie. Alais, in *French Patent No. 759588, British Patent No. 405596*, 1934.
13. H. Hurter, in *British Patent No. 469,361*, 1937.
14. G. Revel, "Aluminium De Haute Purete Obtenu Par Zone Fondue", *Comptes Rendus Hebdomadaires Des Seances De L Academie Des Sciences*, 259 (22), 1964, p.4031.
15. H. Bratsberg, O.H. Herbjornsen, and D. Foss, "Zone Refining of Aluminum", *Review of Scientific Instruments*, 34 (7), 1963, p.777.
16. T. Kino, et al., "Zone-Refining of Aluminum", *Transactions of the Japan Institute of Metals*, 17 (10), 1976, pp. 645-8.
17. W.G. Pfann, "Principleas of Zone-Melting", *Journal of Metals*, 4 (2), 1952, p.151.
18. W.G. Pfann, C.E. Miller, and J.D. Hunt, "New Zone Refining Techniques for Chemical Compounds", *Review of Scientific Instruments*, 37 (5), 1966, p.649.
19. T.A. Engh, *Principles of Metal Refining*. 1992, New York: Oxford Science Publications.
20. A.L Lux, and M.C. Flemings,"Refining by Fractional Solidification", *Metallurgical Transactions B (Process Metallurgy)*, 10B, 1979, pp.71-8.
21. D. Fischer,"A Study on Zone Refining: Solid-Phase Impurity Diffusion and Influence of Separating Impure End", *Journal of Applied Physics*, 44 (5), 1973, pp.1977-82.
22. E.F. Herington,"Zone Refining as a Purification Tool", *Annals of the New York Academy of Sciences*, 137 (Purification of Materials), 1966, pp.63-71.
23. Hashimoto, E., Y. Ueda, and T. Kino,"Purification of Ultra-High Purity Aluminum", *Journal De Physique*, 5 (C7), 1995, pp.153-7.
24. N. Jarrett, et al., *Treatment of Molten Aluminum*, in *U. S. Patent: 3,211,547*, 1965.
25. S.C. Jacobs, *Purification of Aluminum*, in *U. S. Patent: 3,303,019*, 1967.
26. R.K. Dawless, and R.E. Graziano, *Fractional Crystallization Process*, in *U. S. Patent: 4,294,612*, 1981.
27. G.S. Foerster, *Removal of Ni from Molten Magnesium Metal*, in *U. S. Patent: 3,869,281*, 1975.
28. H. Tathgar, *Solubility of Nickel in Mg-Al, Mg-Al-Fe, and Mg-Al-Mn Systems*, PhD Thesis, NTNU, Trondheim, Norway, 2001.